NGU Report 93.089

Landsat TM remote sensing study of geological lineaments on Hinnøya, Vesterålen archipelago, Norway

NORGES GEOLOGISKE UNDERSØKELSE

Postboks 3006 - Lade
7002 TRONDHEIM
Tlf. (73) 90 40 11
Telefax (73) 92 16 20

REPORT

Report no. 93.089	ISSN 0800-3416	Grading: Confidential to 2000

Title:
Landsat TM remote sensing study of geological lineaments on Hinnøya, Vesterålen archipelago, Norway

Author: Bax, Gerhard	Client: Elf Petroleum, Norwegian Petroleum Directorate, Norsk Hydro, Statoil and NGU
County: Nordland, Troms	Commune:
Map-sheet name (M=1:250.000) Svolvær, Narvik	Map-sheet no. and name (M=1:50.000)
Deposit name and grid-reference:	Number of pages: 22 Price: Map enclosures: 1

Fieldwork carried out:	Date of report:	Project no.:	Person responsible:
	09.08.93	61.2574.00	Jan S. Rønning (signature)

Summary:

The geological lineament pattern on the island of Hinnøya, Vesterålen archipelago in Norway, was studied by means of remote sensing techniques. One quarterscene of Landsat TM covering 90 km x 90 km with a spatial resolution of 30 m, registered 900720, was used to extract these structural features. Because of the pronounced topography on Hinnøya it was necessary to correct the apparent strike of the structures with the help of a detailed Digital Elevation Model (DEM) to achive the real orientation (dip) of the lineament producing structures.

Keywords:	Fjernanalyse	
Berggrunnsgeologi		
Forkastning		Fagrapport

Contents

List of Figures

List of Tables

Enclosures

Satellite map (full colour) of the Hinnøya area with imposed geological lineaments

Landsat TM remote sensing study of geological lineaments on Hinnøya, Vesterålen archipelago, Norway

Gerhard Bax
Remote Sensing Laboratory
Department of Physical Geography
Stockholm University
S-10691 Stockholm (Sweden)
Tel.: +46-8-164965
Fax.: +46-8-164818
Internet: bax@natgeo.su.se

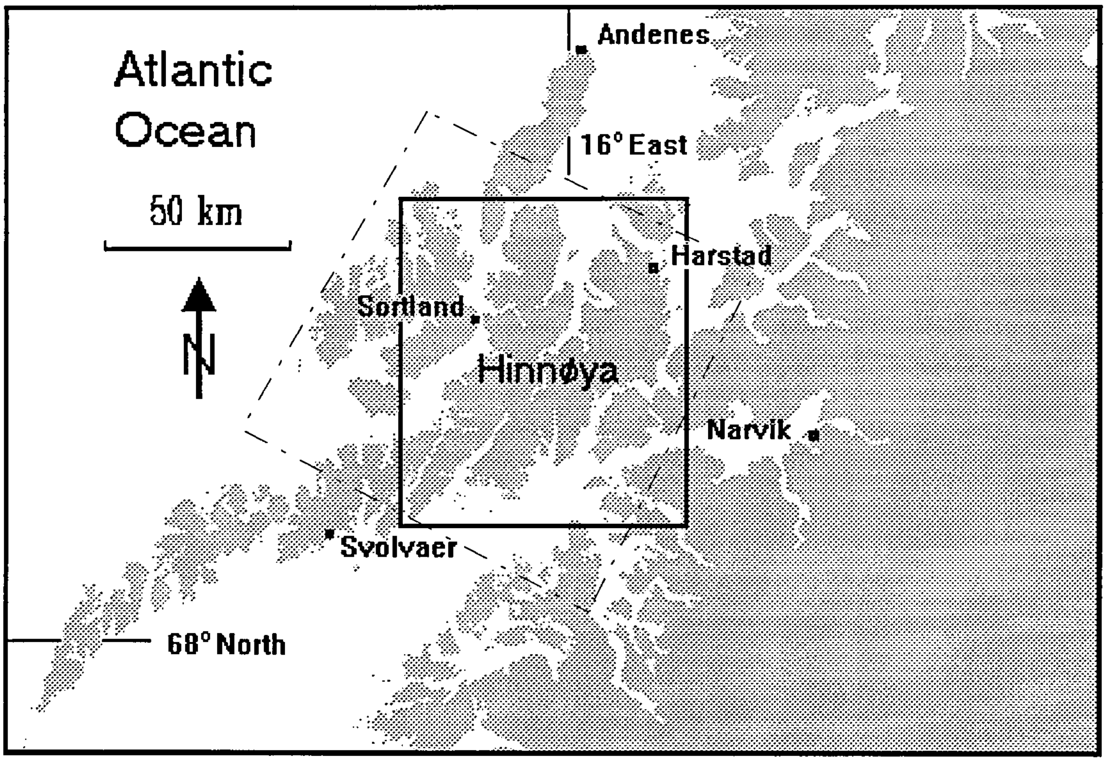

Fig. 1: Location of the study area in northern Norway. The boundary to Sweden, situated in the south-eastern part of the map is not indicated. The dash-dot line represents the coverage of the geo-corrected Landsat TM floating quarter scene, that was acquired for the present study from Satellitbild AB in Kiruna. A skipped version of this image, representing the first principal component of TM 1-5, and 7 is shown in Fig. 3.

1. Introduction

The continental crust, exposed in the archipelago of Lofoten-Vesterålen (cf. Fig. 1) is transected by a large number of fault zones, produced during multi-temporal tectonic activity in the area. At least three tectonic episodes contributed to this pattern.

In Pre-Cambrian times the crystalline rocks of Lofoten were deformed during the crustal amalgamation, that resulted in a Late Pre-Cambrian continent, combining the Baltic and Laurentian Shield.

The Vendian rifting, that opened the ancient ocean Iapetus, contributed together with the Caledonian orogeny significantly to the observed structural pattern. The continental collision between the cratons of Baltica and Laurentia in Palaeozoic times resulted in complicated structural patterns along an at least 5000 km long collision zone. Fragments of this Caledonian-Appalachian continental collision zone, marking the approximate position of the Late Precambrian to Early Palaeozoic Iapetus ocean, were geographically spread during the opening of the northern Atlantic ocean in Tertiary times. One segment of this Caledonian-Appalachian orogen can be found along the north-western margin of northernmost Europe, forming the Scandinavian Caledonides. These Caledonides of north-western Europe suffered no further lateral compression after the Palaeozoic diastrophism and are therefore an excellent example for the study of deformation at deep seated erosional levels.

In association with the opening of the present North-atlantic ocean, several of the older movement horizons were re-activated in accordance to the prevailing stress fields. In many cases new faults developed, were old zones of weakness were lacking. While the two earlier phases of deformation crated both extensional and compressional features, the latest - and still ongoing - episode is **still** entirely dominated by crustal extension.

The geomorphology of northern Scandinavia is a result of (1) the several orogenic cycles outlined above, (2) continental uplift of the resulting craton during the Tertiary, and (3) a final overprint of pre-existing landscapes during several Pleistocene glaciations. In the study area, situated north-west of Narvik (see Fig. 1), a crustal segment representing a Caledonian structural depth of at least 10 km is exposed. Deformation of the involved quartzo-feldspathic rocks started under ductile conditions, and brittle conditions became prevalent when the accretionary wedge had passed the brittle-ductile transition zone on its way onto the underplating continent Baltica. Field studies allow a discrimination of several generations of dislocation zones due to effects of overprinting. At least two generations of faults contributed to the lineament pattern, which is detectable by means of remote sensing. Early - exclusively ductile - structures dip gently to the Northwest and are cut by younger, N-S striking high angle fault-zones showing brittle overprint (pseudotachylite) of initially ductile mylonites. A pronounced topography with fjords that separate steep mountains with elevations up to 2000 m allows a spatial insight in a structural framework, that is a product of polyphase deformation. Lineaments from both the Scandinavian mainland and the Lofoten archipelago were mapped on Landsat TM images. The 3-D orientations of the lineament producing structures were thereafter calculated with the help of a detailed DEM and the obtained results will later be compared with structural measurements from field work.

2. The concept of lineaments

The recognition of large scale linear topographic features in bedrock dominated areas has a long tradition in Scandinavia (Kjerulf 1879, Gabrielsen & Ramberg 1979, Sæther et al. 1991). These surface expressions of geological structures, called lineaments (Hobbs 1912), are important for both pure and applied geoscientific research. Geomorphologic lineaments are traces of plane crustal inhomogenities sculptured by erosion.

Lineament studies can be subdivided into two major groups, depending on the main aim of the investigation. The research can be dedicated to the lineament bounded rock blocks, or the indicated structures themselves can be of interest. Many geomorphologic (Lidmar-Bergström et al. 1991) and geologic studies (Tirén & Beckholmen 1992, Romer & Bax 1992) utilise lineament studies in order to examine the history of the fault bounded blocks. The present study, however, is dedicated to the evaluation of the structural significance of the lineament producing structures themselves.

Lineaments have been extracted from remote sensing imagery of the mountainous study area North-west of Narvik in northern Norway. This area comprises the island of Hinnøya; the largest island of Norway situated in the archipelago of Lofoten - Vesterålen, as well as minor parts of Langøya and the mainland of Norway (cf. Fig. 1).

Fig. 2. Bathymetry and topography around Lofoten-Vesterålen. The grey scale in the image represents ascending elevation of the lithosphere. The image represents an area of 170 km times 130 km with a spatial resolution of 500 m.

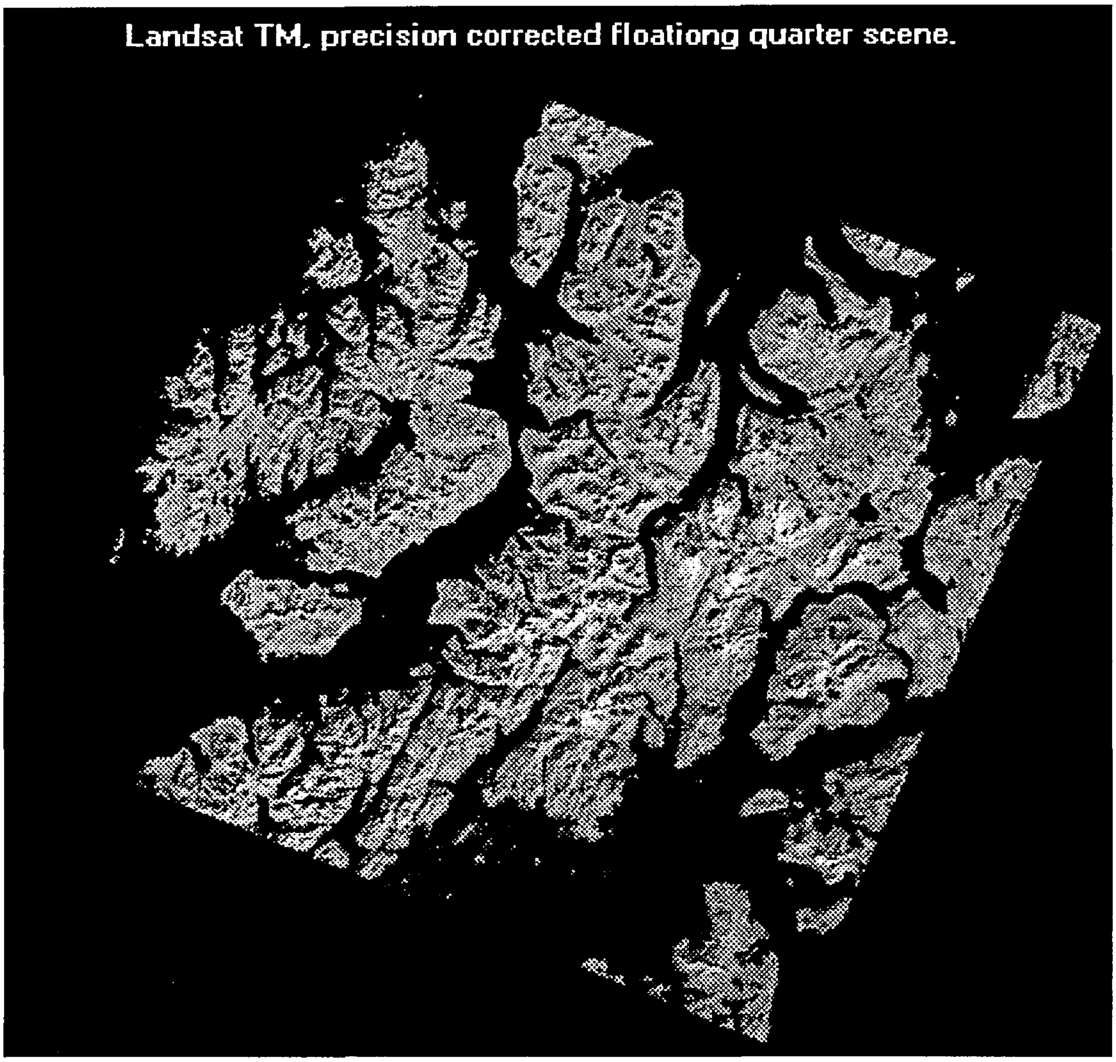

Fig. 3. Geocorrected Landsat TM quarter scene over the study area. Table 1. gives detailed technical information.

Table 1: Technical information about the Landsat image used in this study. The co-ordinate system was changed to the UTM standard ED 50 according to the used DEM.

SCENE ID =199011
ACQUISITION DATE =900720
SATELLITE =L5
INSTRUMENT =TM
PRODUCT TYPE =QUARTER SCENE
TYPE OF GEODETIC PROCESSING =PASS THROUGH
RESAMPLING =CC FALSE
PROJECTION =UTM
USGS PROJECTION # = 9 USGS
MAP ZONE = 33 USGS
PROJECTION PARAMETERS = 0.637838800000000D+07 0.635691200000000D+07 0.999600000000000D+00 0.000000000000000D+00
0.150000000000000D+08 0.000000000000000D+00 0.500000000000000D+06 0.000000000000000D+00 0.000000000000000D+00
0.000000000000000D+00 0.000000000000000D+00 0.000000000000000D+00 0.000000000000000D+00 0.000000000000000D+00
0.000000000000000D+00
EARTH ELLIPSOID =INTERNATL_1909
SEMI-MAJOR AXIS =6378388.000
SEMI-MINOR AXIS =6356912.000
PIXEL SIZE =30.00
PIXELS PER LINE =4180
LINES PER IMAGE =3960
UL 0140020.6460E 690918.5548N 460515.000 7672185.000
UR 0170942.8300E 690840.0018N 585885.000 7672185.000
LR 0170342.3519E 680448.0395N 585885.000 7553415.000
LL 0140306.5469E 680524.5447N 460515.000 7553415.000
BANDS PRESENT =1234567

3. Geology and structural history of the study area

The main part of the area is build up by Precambrian crystalline rocks, that were involved in the Caledonian orogeny about 400 million years ago. The present author (Bax 1989) was able to show that the crystalline rocks exposed in the Rombak area are not autochthonous, but belong to the Lower Allochthon of the Caledonian orogen. This Lower Allochthon was thrusted towards the Southeast during the final stages of the continental collision between the former cratons Laurentia and Baltica. Due to geometrical reasons, also the crystalline rocks on Hinnøya, situated behind the Rombak rocks in terms of thrusting trajectory, have to have an allochthonous position. The crystalline rocks are now exposed in large tectonic windows underneath higher tectonic nappes. These higher tectonic nappes belong to the Middle, Upper and Uppermost Allochthons of the Caledonian orogen. In the Hinnøya area, a minor region south of Harstad is built up by remnants of these higher nappes (Björklund 1989).

The structural history of the Hinnøya area is quite complicated. Parts of the crystalline rocks probably suffered deformation during Pre-Caledonian orogenies almost 2 billion years ago. Most of the structures relevant to the present study were, however, formed during the Caledonian orogeny. During this episode of deformation, the rocks along the former continental margin of Baltica were telescoped and thrusted onto each other in a piggy-back style. This means that first the highest nappe was thrusted onto the underlying rocks, and the active thrust plane moved stepwise deeper into the continental crust of Baltica. In other words; the thrust plane underneath the crystalline rocks of the Lower Allochthon is younger than that one on top of them.

In and around the comparable Rombak area (Bax 1989), at least five phases of deformation were distinguishable. The recognition of two of these was important for the purpose of lineament interpretation. The deformation phase D_3 resulted in ductile, relatively flat towards NW dipping shear zones. The slightly younger D_4, however, formed when the accretionary wedge passed the ductile - brittle transition zone, permitting the percolation of fluids. D_4 -structures strike approximately North-South with steep dips towards either East or West. Along the fault planes occurrences of pseudotachylite can be observed, overprinting more ductile mylonites. At many places huge quartz veins bounded by D_4-structures can be observed.

4. Recognition of linear features

In the above outlined lineament concept we focused on geological lineaments. Due to the mountainous character of Hinnøya, the human influence is more or less restricted to the coastal areas and the major valleys, and the few power lines crossing the areas can be extracted from the topographic maps. Where present, the soil and vegetation layer is usually very thin, and almost all linear features can be explained by elongated inhomogenities in the bedrock.

Many of the lineaments represent surface expressions of mappable faults, other visualise lithological inhomogenities like compositional layering. In many cases, pronounced lineaments can be extracted directly from detailed topographic maps or Digital Elevation Models (DEM). Other possibilities are to investigate images, in our case a digital Landsat TM scene with 7 spectral bands, to detect lineaments. To use digital imagery has several advantages. The different wavelength bands can be combined, and each of them enhanced to obtain a satisfying results for just this area. It is impossible to give general recommendations. Every area is different, and even the same area will show seasonal variations depending on the time of image registration. The procedures used in this study are outlined in the following chapters.

5. Data sources

One floating quarter scene Landsat TM (acquisition date 1990 07 20) geocorrected according to UTM zone 33 W was used for the present study . The passive sensors of the land observation satellite Landsat TM show the reflected sunlight with a spatial resolution of 30 m in 6 wavelength bands (TM 1-5, and TM 7) plus 1 thermal wavelength band (TM 6) with 120 m spatial resolution. Information from all 6 bands with 30 m resolution was used in this study.

A digital terrain model with 100 m resolution in the horizontal plane, and 7.5 m vertical resolution was used. The original vertical resolution was much higher, but for reasons of data storage and handling (1 pixel per byte = 256 levels) this for the study sufficient resolution was chosen.

6. Data processing

Different band combinations, and band ratio combinations were tested during the initial phase of this study. As the main aim of investigation was to extract the major lineaments on Hinnøya, the first principal component (PC 1) of the 6 bands with 30 m resolution was regarded as sufficient. A further treatment with an edge enhancement algorithm (3 x 3 window with a kernel -1,0,-1, 0,5,0, -1,0,-1) was applied to a selected part covering the island of Hinnøya. This part of the image had 2333 columns and 2666 rows ranging in W E direction from 498 000.0 to 567 990.0, and in S N from 7 572 010.0 to 7 651 990.0 (69 990 m $*$ 79 980 m). The original data were accompanied by a file documentation (Table 1), determining the corners of the image (upper left 460500;7672200, lower right 585900;7553400). A comparison with recognisable features (small island, significant coast structures) in both the DEM and the topographic map of Norway (1 : 50 000) showed however and error corresponding to approximately 500 m lateral distortion. This "error" was due to two different UTM projections (ED 50 and WGS 84), that was easily fixed by correcting the co-ordinates for the origo. After this treatment, the positions of more than half a dozen control points were estimated with pixel resolution. This precision was necessary to allow overlay analyses. It would have been possible to resample to any of the two projections, but resampling procedures change the textural features of an image, depending on the applied interpolation algorithm. For visualisation on the enclosed, large scale colour out print, a slightly different enhancement technique was used. To obtain reasonably "natural" colours, TM 5 is displayed in red, TM 4 in green, and TM3 in blue. A "stronger" Laplace filter was necessary to enhance the linear features in this band combination. I used the following kernel in a 3 x 3 window: -1,-1,-1, -1,12,-1, -1,-1,-1.

The DEM was used for several purposes. In an initial phase of the study, I tried to extract linear features with a by me specially developed "trench detecting algorithm". This treatment failed however on the available DEM, although it showed good results in "synthetic" data. Later treatments with gradient filters showed a diagonal SW-NE striping, which probably caused the confusion for my algorithm. During the following stages of the study the DEM was used to extract the z co-ordinates (elevations) of lineament nodes for 3D, as well as for slope and aspect calculation. The striping was reduced for these purposes with smoothing procedures.

7. Geometrical aspects of lineament producing structures

There are different problems when trying to apply the results of lineament studies in areas with pronounced topography. In areas with lack of topography, in other words totally flat areas, the trend of any linear feature corresponds to its geological strike. This is simply because the definition of geological strike is the intersection of a given structure with a horizontal plane. The other extremes are vertical structures. These structures are always projected into the map plane showing their real strike. In all other cases, any existing topography will influence the trace of any non-vertical structure in the map projection.

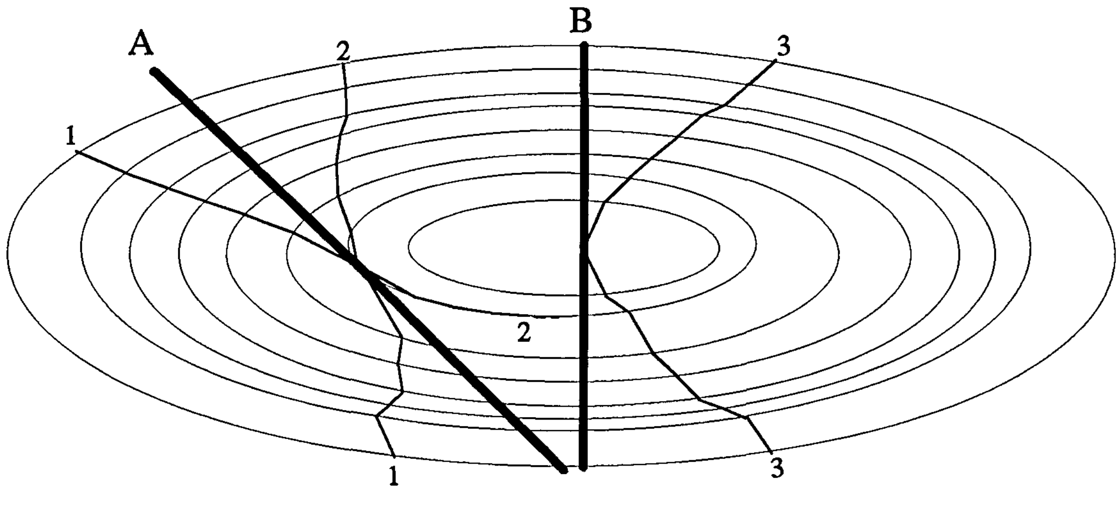

*Fig. 4: Some examples of different geometries in map projection of an elongated hill. The thick, oblique line [**A**] to the left illustrates the case of a geological strike oblique to topographic features. In this oblique case the geological structure can either dip towards the same hemisphere as the topography [1] or towards the hemisphere that is situated upslopes [2]. Here the maximum angle of difference [illustrated by 2] is equal to that one between dip of the structure and slope of the topography. The other case [**B**] represents the special case of a rectangularity between slope and dip. The traces of the structures are kept straight between the elevation contours, illustrating constant slope between the contours.*

The distorting effect of pronounced topography on the apparent strike of lineaments has been neglected by most lineament studies in the literature. As long as relatively flat areas are examined on regional scale, this error is in fact in many cases negligible. The risk for distortion increases with the "spatial resolution" of the interpreted imagery and the fractal dimension ("roughness") of the topography at the scale of observation. As shown below (Fig. 4), there are several geometrical parameters that influence the degree of distortion. The basic concepts for the following equations are explained in textbooks concerning structural geology (Turner & Weiss 1963, Ragan 1985, Wallbrecher 1986). The differences[ϑ] between real (geological) strike of a structure [σ_S] and the projection of its trace into the horizontal map plane (apparent strike [σ_{App}]) can be easily calculated if the following 4 parameters are known.

α_T: Dip direction of the topography (aspect)
φ_T: Inclination of the topography (slope)

α_S: Dip direction of the geological structure
φ_S: Inclination of the geological structure

For the calculation of the line of intersection between the two planes with the dip vectors (φ_T/α_T and φ_S/α_S) it is necessary to use the normal vectors of these planes. All four values are easily derived, as the orientation of the plane normal vectors (φ_{Tn}/α_{Tn} and φ_{Sn}/α_{Sn}) can be easily derived from the dip vectors by the following equations (Wallbrecher 1986).

$$\alpha_{Tn} = \alpha_T + 180; \quad \varphi_{Tn} = 90 - \varphi_T; \quad \alpha_{Sn} = \alpha_S + 180; \quad \varphi_{Sn} = 90 - \alpha_S$$

The apparent strike [σ_{App}] of a geological structure can be derived as follows.

$$\sigma_{App} = \arctan \frac{\sin\varphi_{Tn} \cdot \cos\alpha_{Sn} \cdot \cos\varphi_{Sn} - \cos\alpha_{Tn} \cdot \cos\varphi_{Tn} \cdot \sin\varphi_{Tn}}{\sin\alpha_{Tn} \cdot \cos\varphi_{Tn} \cdot \sin\varphi_{Sn} - \sin\varphi_{Tn} \cdot \sin\alpha_{Sn} \cdot \cos\varphi_{Sn}} \qquad (1)$$

In our case, where only the difference between the strikes is relevant, we can substitute the dip direction value of one of the planes (for example [α_{Sn}]) with **0** to simplify the calculation. The angular difference to the aspect of the topography [δ_{ST}] should then be substituted for the real aspect [α_{Tn}]. The trace of north dipping geological structures (dip direction = **0**) will be influenced by pronounced topography according to the following formula.

$$\sigma_{App} = \arctan \frac{\sin\varphi_{Tn} \cdot \cos\varphi_{Sn} - \cos\delta_{ST} \cdot \cos\varphi_{Tn} \cdot \sin\varphi_{Tn}}{\sin\delta_{ST} \cdot \cos\varphi_{Tn} \cdot \sin\varphi_{Sn}} \qquad (2)$$

We have now received σ_{App} which represents the difference in dip direction between the real dip of a geological structure (in our case 0) and the trend of its trace in map projection. This trend is in lineament studies assumed to represent the strike of a structure. According to definition, the strike line of a geological structure and the azimuth of the dip are perpendicular to each other. As outlined earlier, σ_{App} can not exceed 90° ($0 < \sigma_{App} < 90$). As the relationship between σ_{App} and ϑ can be expressed in the following way,

$$\textbf{arctan}\,\vartheta = \textbf{arctan}\frac{1}{\delta_{App}} \tag{3}$$

There are still 3 variables left in (3), which makes it impossible to present ϑ in a simple Cartesian x, y, z diagram. In the 2 diagrams of Fig. 5 the value of ϑ is shown for 2 constant values of δ_{ST}. One intermediate case A [$\delta_{ST} = 45$], and one extreme case B [$\delta_{ST}=90$].

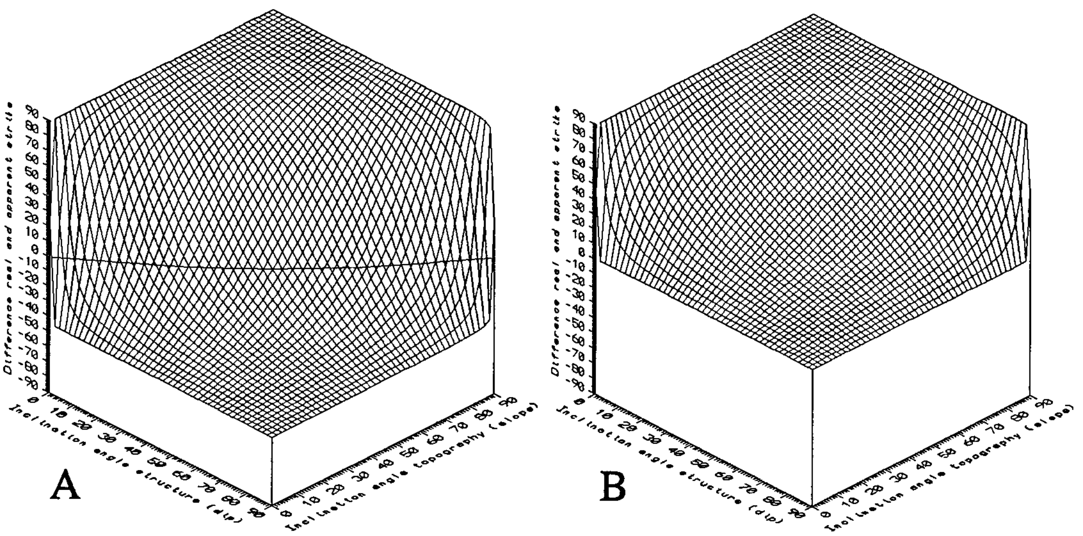

Fig. 5: Difference between real and apparent strike as a function of geological dip and topographical slope. The left diagram shows an intermediate state with an angle of 45 º between dip and slope, and the right diagram illustrates the relationships for the case that dip and slope are perpendicular. The horizontal line in A *represents an* ϑ *of 0. Negative values of* ϑ *represent cases like 2 in Fig. 4. Compare both diagrams with the cases illustrated in Fig. 4.*

8. The 4 dimensions of geological structures

As shown above, a three dimensional structural framework can be derived from a two dimensional lineament pattern if the differences in elevation are known along the exposure of the structure. The fourth dimension, the time of creation of these structures, is not so easy to derive by means of geometry, but several hints can be deduced from the lineament pattern to establish a relative chronology.

Older structures are always cut by younger ones, if the younger movements establish new faults. The lineament pattern of a polyphase deformation should therefore contain young, long, continuos lineaments disrupting older ones. These older structures become disrupted, and their uninterrupted length is therefore shortened. One major problem with this method is that pairs of tapering shear zones very often show asymptotic geometries close to their junctions, and it is therefore often difficult to decide which one cuts the other one.

Age relationships established from remote sensing studies should in any case be verified by detailed field work at critical lineament junctions. In many cases these observations can also give new information about the trajectories of the adjacent fault bounded blocks. Slickensides and sometimes even shear sense indicators (cf. Simpson and Schmid 1983) can help to establish a chronology.

In the Rombak area, the geometrical relationships between several generations are known (Bax 1989). Of interest for the purpose of the gold prospecting (cf. Bax et al. 1991) were at least 2 of 5 generations. Generation D_3, whose structures were formed during the updoming of the antiformal stack (cf. Romer & Bax 1992), is represented by low angle ductile shear zones dipping towards the Northwest. These types of structures had to be avoided for the purpose of prospecting, as ductile shear zones are essentially impermeable for ore bearing fluids. The slightly younger D_4-structures, however, were formed when the accretionary wedge migrated upwards along its floor thrust passing the ductile-brittle transition zone.

The time aspect gives us the fourth dimension of lineament analysis. This is a very important aspect of structural studies, but very often a neglected one. It will in any case lead to erroneous results if lineament trends will be used to describe paleostress in an area, assuming contemporaneous faulting. On the other hand, not every discernible lineament direction represents alone a specific phase of deformation. Very often a rhombohedral pattern can be observed (Romer & Bax 1992). To discern lineaments producing structures not only the strike but also the dip has to be considered.

9. Results

The above described methods were applied on a Landsat TM image over the study area. The methodology is a combination of remote sensing and GIS techniques. Whenever necessary, slight modifications of proven procedures were applied to enhance the desired results.

All lineaments were interpreted manually. This brings in a human factor that varies in many respects, even though the interpreter in all cases was the present author.

Several attempts were made during the study to apply automatic lineament detection. Both image analysis techniques on remote sensing imagery (Lundén et al. 1990, Wester et al. 1990) and those applied to Digital Terrain Models were tried (cf. Eliason & Thiessen 1986). The anastomosing pattern derived from satellite imagery by line detection techniques is very difficult to interpret. I found it only useful in comparison with manually interpreted patterns. In an early phase of the study I developed a new technique (Bax, unpublished results) to "look" for typical topographical features characterising geomorphologic lineaments. The technique worked well with artificially created elevation grids. With the elevation data available, it failed however. Simple gradient filtering of the raster DEM showed an intense diagonal striping in the data set. This artefact appeared probably due to interpolation techniques from one co-ordinate system to another.

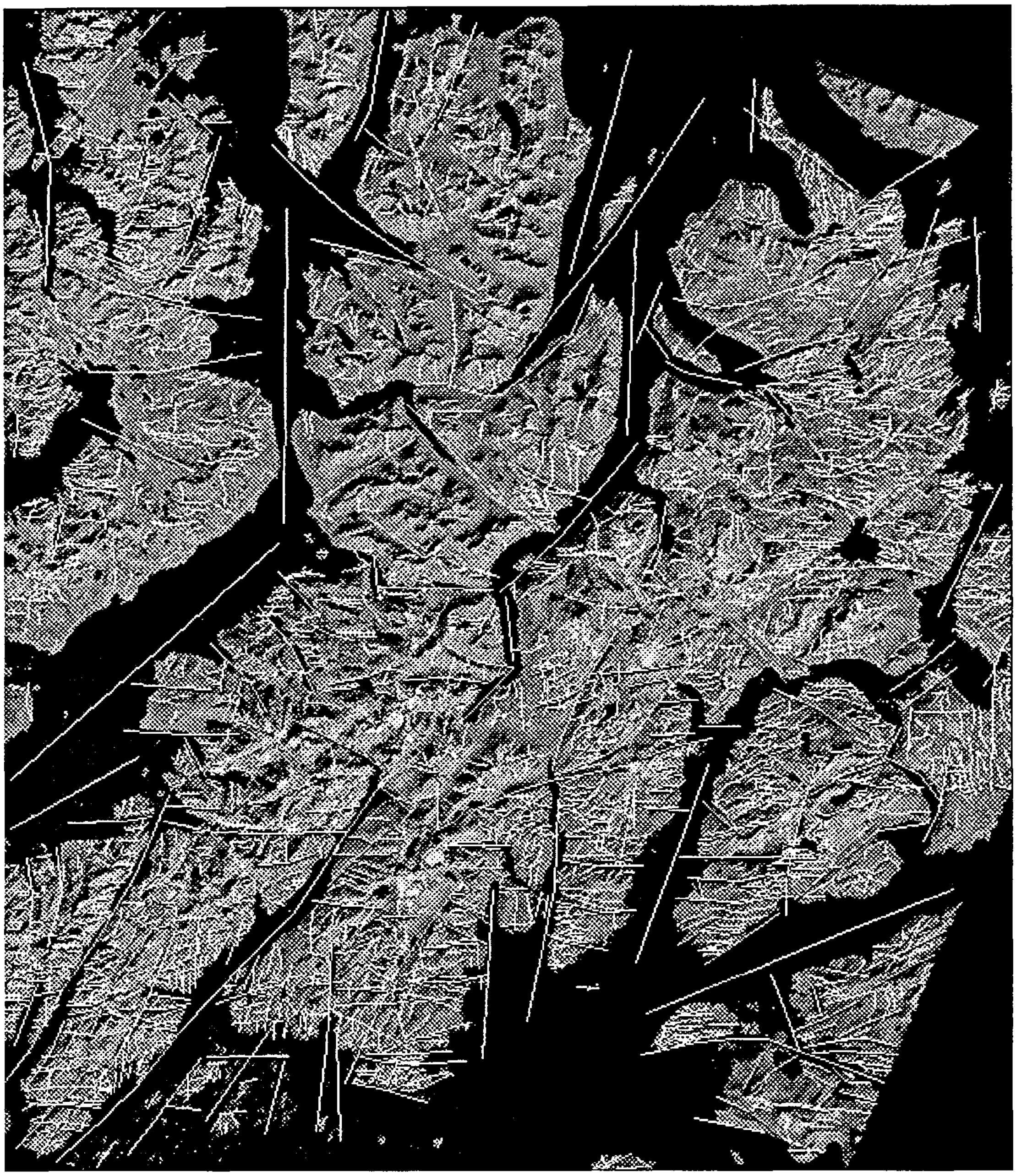

Fig. 6: Extracted area for lineament interpretation. Edge enhanced first principal component out of bands 1-5, and 7. Skip factor 4. Lineaments are transformed from vector to raster format and draped over the image with the highest digital value (255). For scale see next Figure.

The next step in the study was to correct all lineaments with the help of a DEM to receive both real strike and dip. We have to keep in mind that large errors in dip and strike will occur, if the aspect and slope values of the topography are relatively constant along a lineament.

Although a series of errors can occur in 4-D lineament analysis, this technique can give much new information about the structural history of an area. Many of the above mentioned possible errors can be avoided, if the method is used with care. An unrenouncable prerequisite for a meaningful calculation is an exact geo-coding of all input data.

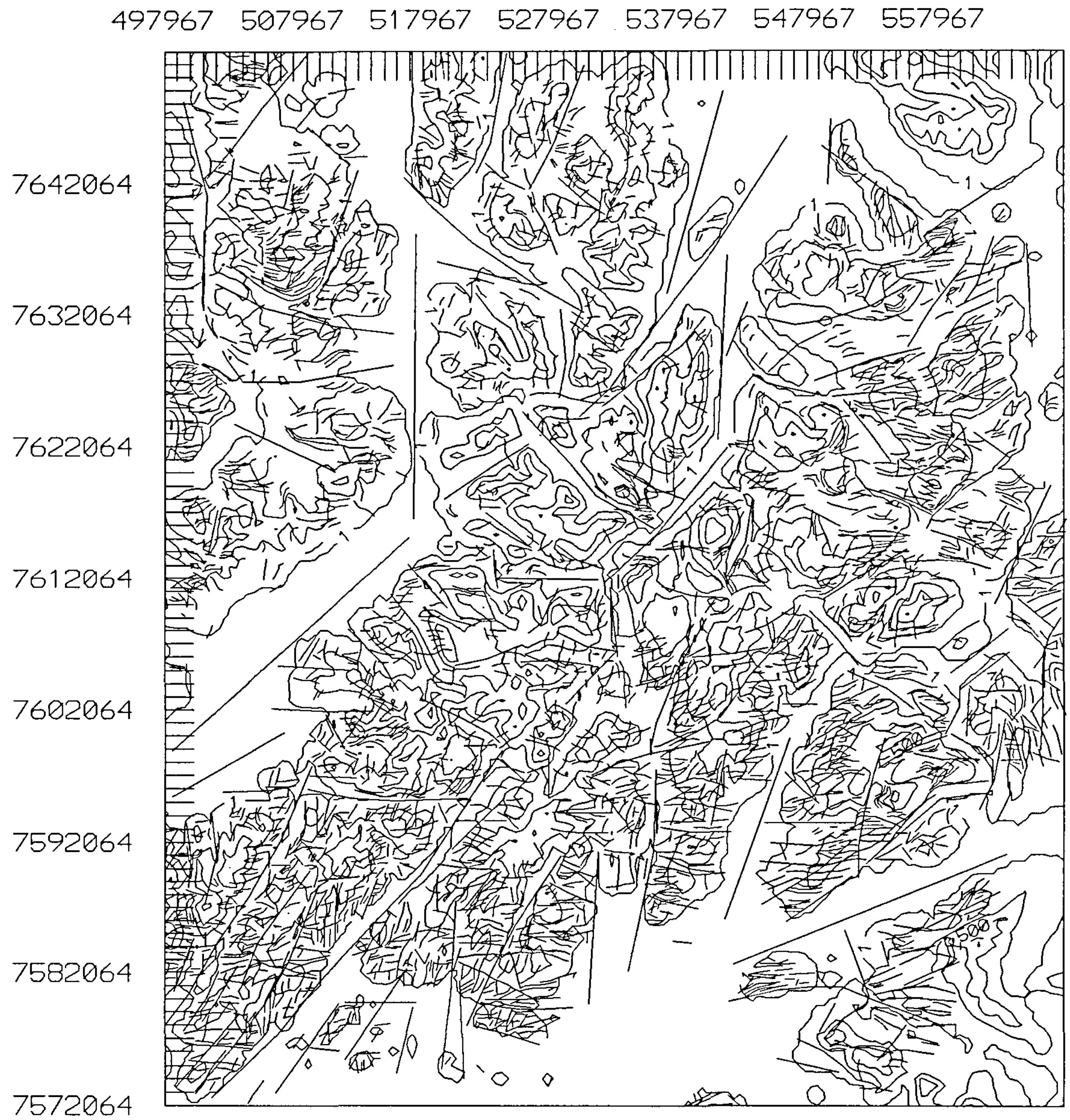

Fig. 7 Result of the lineament interpretation on the island of Hinnøya. This figure shows the interpreted lineaments draped over a topographic map with an equidistance of 250 m. The numbers to the left and above the map are the co-ordinates in the UTM grid 33 W. Tic lines every km.

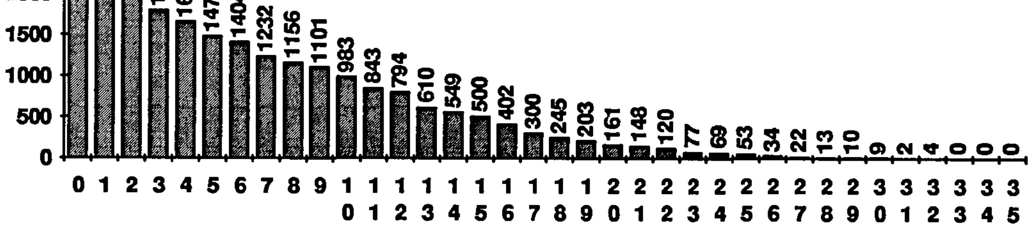

Fig. 8:. Inclination of segments (> 100 m) of the lineaments from the Hinnøya area. 2482 segments are horizontal, and 4 are as steep as 32 degrees.

Fig. 9. Calculated dip of lineament segments that were interpreted from Landsat imagery. The elevations at the nodes were used to calculate the dip of every single segment. Compare with the location of the lineaments in the previous figure.

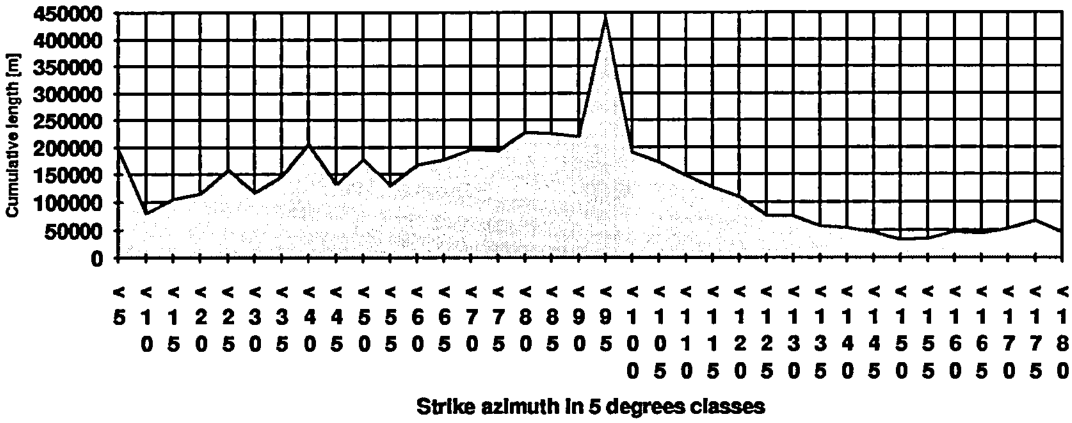

Fig 10: Cumulative length of lineament segments for 5 degree's classes in meter. The total length of all 2760 lineaments was 4 802.265 km.

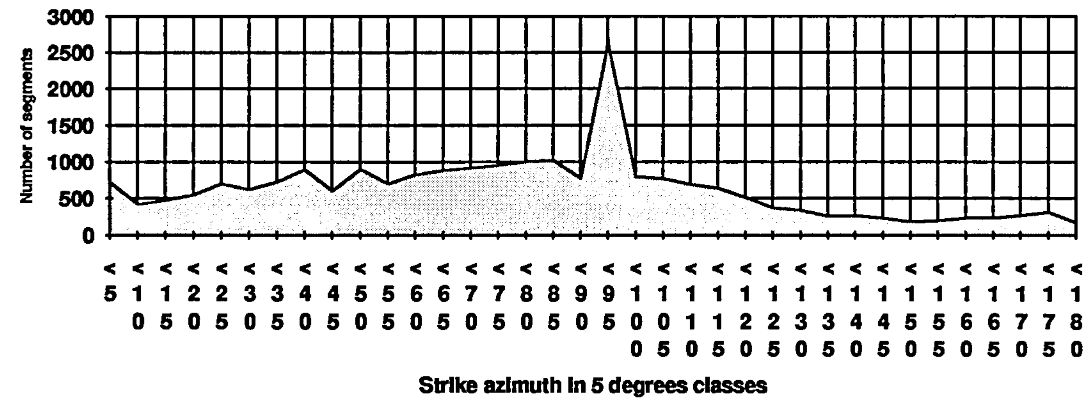

Fig 11: Number of lineament segments plotted regardless of their total length. The total number of segments was 22 879 in 2760 lineaments.

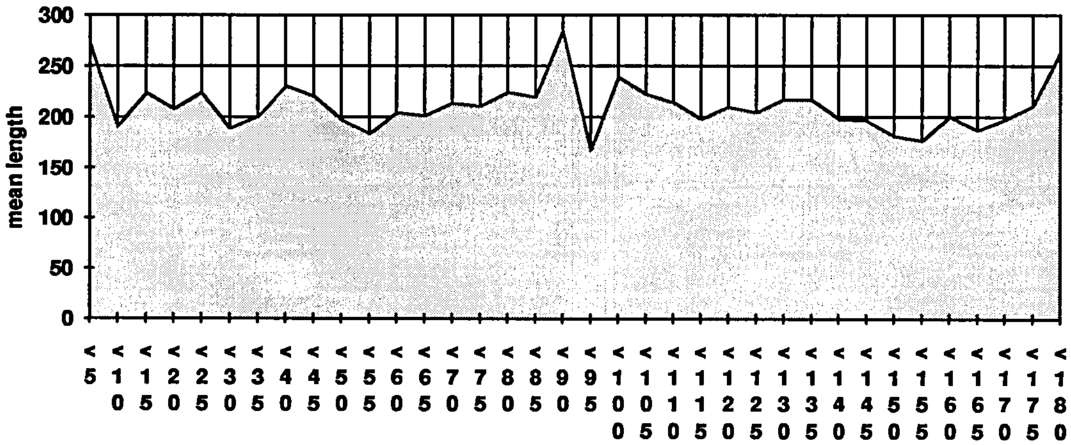

Fig 12: Mean length of all lineament segments. This diagram shows that that the mean length of the lineament segments is about 200 m. As lineaments are segmented by the interpreter, mean length is often a more psychological factor than a geological one. The quite even distribution of segments shows that I did not favour any direction besides a slight over-representation of the E-W direction. The mean length can, however, also be seen as an indicator how straight a lineament is. Here, all directions had similar amounts of curvature

Finally, I tried to correct the apparent strike (trend in the map projection) with the help of the DEM to receive the real (geological) strike. One of these examples is shown below.

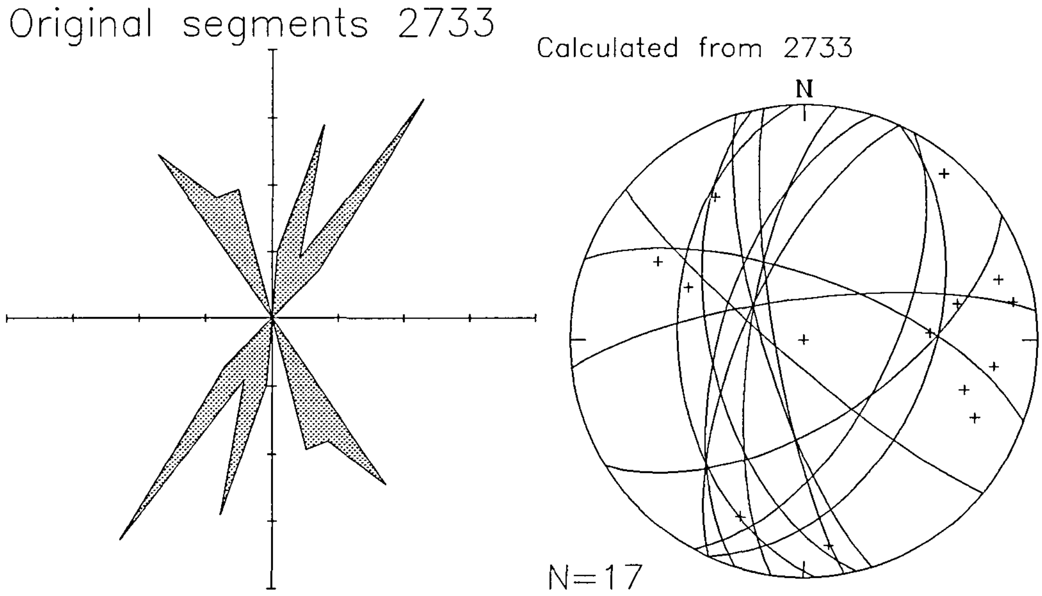

Figure 13: Left: Rose diagram of the observed trends. 1 Tic = 1 observation. Right: Schmidt net, lower hemisphere. Calculated orientation shown in both great circle and normal vectors. Observed trend (left) and calculated, real strike and dip (right) of a lineament (called 2733) containing 17 segments (Four of the calculated dips are vertical and plot therefore in the centre of the hemisphere). The comparison of these two diagrams shows best the advantages of the 3-D method. Plots of the observed trends of lineaments tend very often to have two maxima.

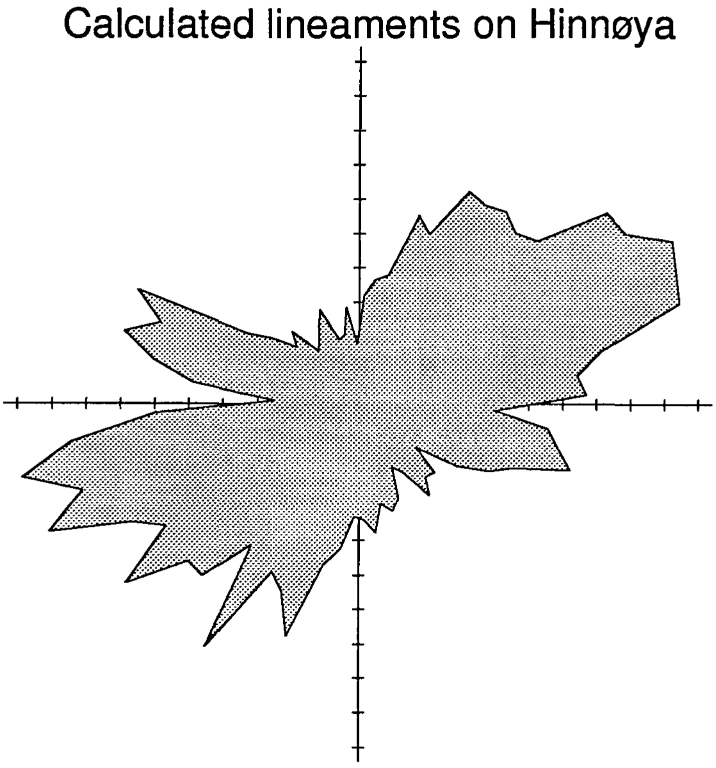

Fig 14: Rose diagram of the dip directions of lineament segments that were mapped on Hinnøya. Ticks along the axes represent a frequency of 10 segments each.

10. Conclusions and recommendations

The structural history of an area can only be derived in combination with detailed field observations. The lineament interpretation with remote sensing techniques can help to concentrate the fieldwork on a few critical localities. With the knowledge from the field work, reappearing textural patterns in the imagery can be interpreted with much higher confidence.

Many possible aspects of this study, like comparisons of the interpreted structures with published geological maps and 3D modelling remain still to be done. I hope to complete the present fragment in the future.

11. Remarks and acknowledgements

The study on Hinnøya would have been impossible without the close co-operation with other colleagues working in these areas. My special thanks go to Odleiv Olesen and Einar Tveten at NGU. At the Remote Sensing Laboratory in Stockholm, the fruitful discussions with Bengt Lundén, Kjell Wester and many other contributed a lot. The Swedish Space Corporation supported during the initial phase parts of the present study. Due to my position as a researcher depending entirely on project money, most of the study had to be carried out while I was unemployed, as none of the asked research councils supported this project during its main phase. This fact was naturally limiting my encouragement in the study. I appreciate very much Leif Wastensson's allowance to use the computer facilities of the Remote Sensing Laboratory at Stockholm university. Odleiv Olesen helped me to finance the necessary fieldwork, costs in connection with meetings and minor hardware requirements. I would like to thank Odleiv Olesen and Christine Fichler for their hospitality during my visits in Trondheim.

12. References

Bax,G. 1989: Caledonian structural evolution and tectonostratigraphy in the Rombak-Sjangeli Window and its covering sequences, northern Scandinavian Caledonides. *Nor. geol. unders. Bull.*415, 87-104.

Bax, G., Lundén, B., Wester, K. & Romer, R.L. 1991: Remote sensing techniques as mineral exploration tools in the Scandinavian Caledonides and their Fennoscandian foreland. *Proceedings of IGARSS'91 Symposium,* Helsinki, June 3-6, 1991

Björklund, L., 1989. *Geology of the Akkajaure-Tysfjord-Lofoten traverse, N. Scandinavian Caledonides.* Ph.D. thesis Gothenburg, Geologiska Institutionen, Publ. A 59, 214pp.

Davis, J.C., 1986: *Statistics and Data Analysis in Geology.* Wiley, 646 p.

Eliason, J.R. & Thiessen, R.L. 1986: Geologic spatial analysis: a new multiple data source exploration tool. *5th them. conf.:Remote sensing for exploration geology. Reno, Nevada,*Sep 1986,677-692

Gabrielsen, R.H. & Ramberg, I.B. 1979: Fracture pattern in Norway from LANDSAT imagery: Results and potential use. *Proc. Norwegian Sea Symp., Tromsø, Norw. Petrol. Soc. 1979, NSS/11,* 1-20.

Hobbs, W.H. 1912: *Earth features and their meaning.* Mac-Millian Co, New York, 506 pp.

Kjerulf, T., 1879: *Udsigt over det sydlige Norges geologi.* W.C. Fabritius, Christiania. 262 pp.

Lidmar-Bergström, K., Elvhage, K. & Ringberg, B. 1991: Landforms in Skåne, south Sweden. *Geografiska Annaler. 73 A (1991) 2, 61-91.*

Lundén, B., Wester, K. & Bax, G. 1990: Landsat-TM for geological mapping in Saudi Arabia. *Swedish Space Corporation,* **FUX 810-02.**

Mardia, K.V., 1972: *Statistics of Directional Data.* Academic Press.

Marshak, S., & Mitra, G., 1988: *Basic methods of Structural Geology.* Prentice Hall.

Romer, R., & Bax, G., 1992: The rhombohedral framework of the Scandinavian Caledonides and their foreland. *Geologische Rundschau,* **81/2**, 391-401.

Ragan, D.M., 1985: *Structural Geology, An Introduction to Geometrical Techniques,* Third Edition: John Wiley & Sons, 393 pp.

Sæther, B.M., Rueslåtten, H.G. & Henningsen, T.H. 1991: Advanced techniques for lineament analysis. *Paper presented at the Eight Thematic conference on Geologic Remote Sensing, Denver, Colorado, USA, April 29 - May 2, 1991.*

Simpson, C. & Schmid, S.M., 1983: An evaluation of criteria to deduce the sense of movement in sheared rocks. *Bull. geol. Soc. Am.*, Vol. **94**, 1281-1288.

Tirén, S.A. & Beckholmen, M., 1992: Rock block map analysis of southern Sweden. *Geologiska Föreningens i Stockholm Förhandlingar,* Vol. 114, Pt. 3, pp 253-269.

Turner, F.J., & Weiss, L.E., 1963: *Structural Analysis of Metamorphic Tectonites.* McGraw-Hill, 545 p.

Tveten, E. & Zwaan, B. 1993: Geology of the coast-region from Lofoten to Loppa, with special emphasis on faults, joints and related structures. *NGU report No.* **93.083**, 25pp.

Wallbrecher, E., 1986: *Tektonische und gefügekundliche Arbeitsweisen: graphische, rechnerische und statistische Verfahren.* Enke Verlag, 244 p.

Wester, K., Lundén, B. & Bax ,G. 1990: Analytically processed Landsat TM images for visual geological interpretation in the northern Scandinavian Caledonides. *Journal of Photogrammetry and Remote Sensing* **45**, 442-460.

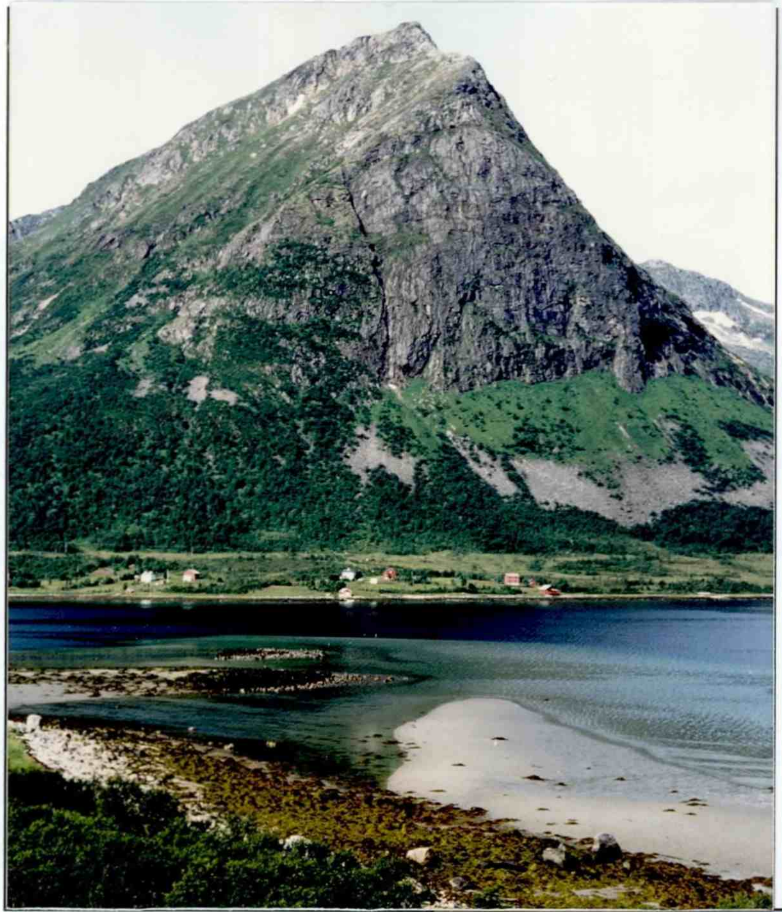

Fig. 15 (left): Lineament contact between gneiss and granit at Röyrtinden (749 m), Godfjorden. Picture looking W from Björnrå.

Fig 16: Lateral branch of the Gullesfjord lineament (see also figure 14 in Tveten & Zwaan 1993). Like many other main shear zone the Gullesfjord fault is braching out laterally leading to an anastomosing lineament pattern. Locality 1 km north of the peak of Rundskardtindan. Picture looking N with Forøya in the background.

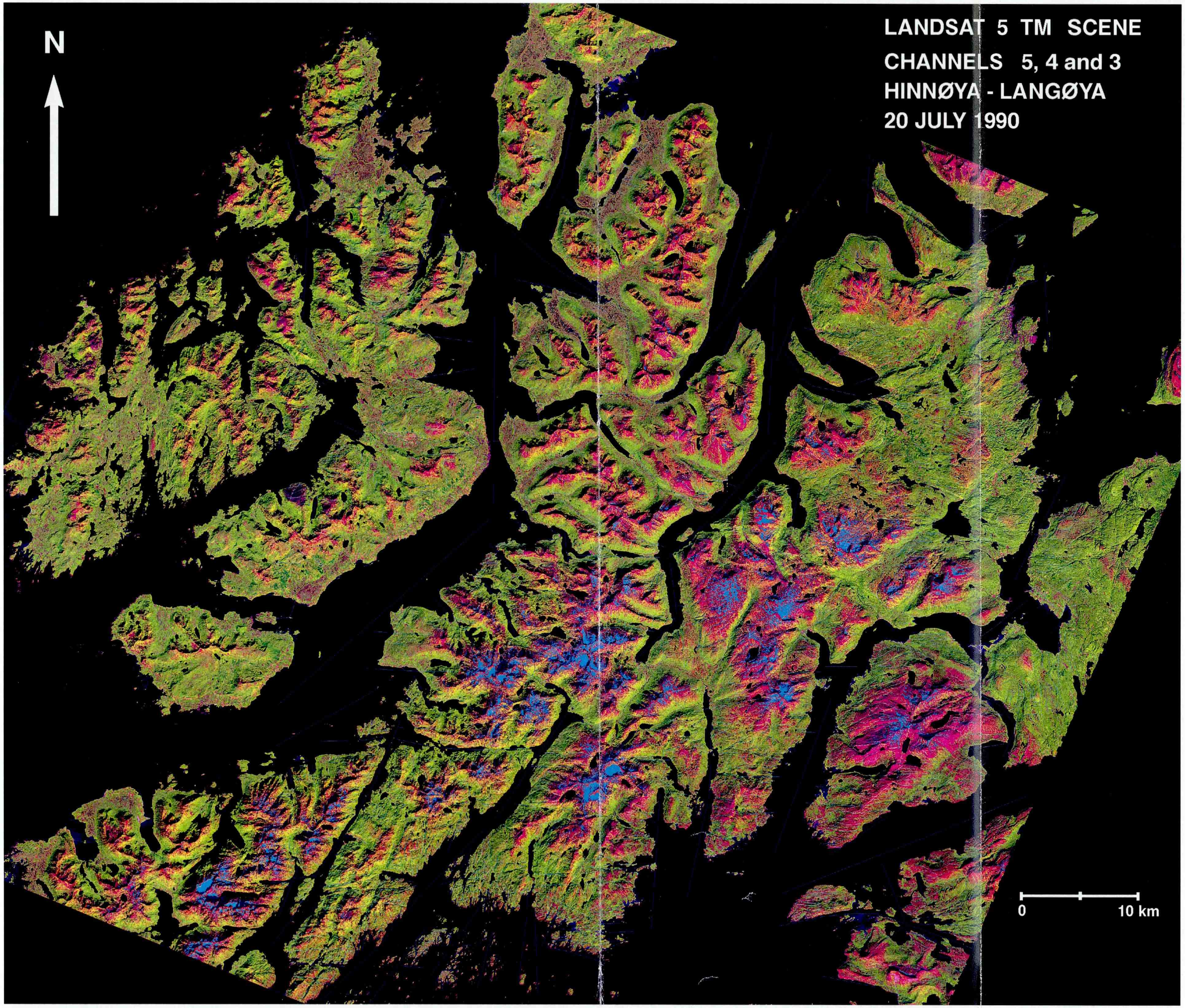
N
LANDSAT 5 TM SCENE
CHANNELS 5, 4 and 3
HINNØYA - LANGØYA
20 JULY 1990
0
10 km